Proc. Natl. Acad. Sci. USA
Vol. 94, pp. 3504–3506, April 1997
Chemistry

Chlorophyll *a* dimer: A possible primary electron donor for the photosystem II

S. BOUSSAAD, A. TAZI, AND R. M. LEBLANC*

P.O. Box 249118, Department of Chemistry, University of Miami, Coral Gables, FL 33124-0431

Communicated by Joseph J. Katz, Argonne National Laboratory, Argonne, IL, January 27, 1997 (received for review November 1, 1996)

ABSTRACT **In the photosynthetic membrane, there is a particular aggregated state for the chlorophyll *a* (Chl *a*) molecules with a specific arrangement responsible for the high efficiency of energy conversion. Chl *a* monolayers, transferred onto solid substrates, are systems that potentially can mimic the packing of the *in vivo* system. The association of Chl *a* in the monolayer results in the formation of dimers with an average size of 3.00 ± 0.15 nm. Considering the organization of the dimers, we assume that P680 is a dimer with the (anti) parallel transition moments of the constituent. The Chl *a* macrocycles most likely are tilted to each other by 30° with respect to the membrane plane.**

Green plants use light energy, through photosynthesis, to reduce CO_2 and produce carbohydrates. The central unit where this activity takes place, the photosynthetic membrane, is described as a segment of lipid bilayer in which protein–pigment complexes are bound. Two complexes within the photosynthetic membrane are considered the key reaction centers, photosystem I (PS I) and PS II (1). Pigments, such as chlorophyll *a* (Chl *a*), located within PS I and PS II, play a major role in the capture of light energy and the subsequent charge transfer that results in CO_2 reduction (2). Chl *a* has a broad absorption spectrum, and aggregation through self-assembly typically leads to changes in its optical properties (3, 4). Red shifts are commonly observed in *in vitro* Chl *a* systems, such as thin films, monolayers, and colloidal dispersions, used as models for the *in vivo* system (5). One such system, based on the Langmuir–Blodgett (L–B) (6) technique for forming ordered thin films, allows the orientation of molecules in a molecular monolayer at an air/water interface and the subsequent transfer onto solid substrates. The transferred L–B film is highly packed and well organized, and the use of this technique allows preparation of systems to potentially mimic the *in vivo* packing of Chl *a* within the photosynthetic membrane.

Numerous attempts have been made to model the arrangement of Chl *a* to rationalize its high energy conversion efficiency. One model (7) proposed for the primary electron donor of PS I describes the formation of a Chl *a* dimer held together via water bridges. In this model, the oxygen of one H_2O molecule is coordinated to the magnesium of a Chl *a* molecule, while its hydrogen bonds to the keto carbonyl group of a second Chl *a* molecule. A second H_2O molecule completes the dimer in the same way. This results in a structure where the distance between the Mg centers is 0.89 nm, and the interplanar separation between the macrocycles is 0.36 nm.

In an effort to obtain direct structural information on the aggregation of Chl *a* in thin films, we have examined monolayers of Chl *a* transferred onto freshly cleaved graphite (HOPG, ZYB grade, Advanced Ceramics, Lakewood, OH) by scanning tunneling (STM; Nanoscope II STM, Digital Instruments, Santa Barbara, CA) (8, 9) and atomic force (AFM) (10, 11) microscopies, i.e. scanning probe microscopy. Chl *a* (Trifolio-M, Lahnau, Germany) was dissolved in benzene at a concentration of 2×10^{-1} g/liter and spread at the air/water interface of a homemade trough using a phosphate buffer (pH, 8) as the subphase. The monolayer was compressed at a speed of 2 $Å^2 \times \text{molecule}^{-1} \times s^{-1}$ and transferred onto graphite at a surface pressure of 20 mN/m by vertical dipping and rising at 2 mm/min.

Fig. 1*a* shows an STM image (214.5 × 214.5 nm) of the Chl *a* monolayer where one can easily see the L–B film boundary. In the upper portion of this image, one can observe that Chl *a* grains are well organized, and in the lower portion, the graphite structure, which is shown in detail in Fig. 1*b*. The STM image in Fig. 1*c* (70 × 70 nm) shows at higher resolution the organization of the grains and their boundaries. This particular type of STM image is an indication of the uniform distribution of the charge density in the L–B film. The image of Fig. 1*d* (35 × 35 nm) shows grains packed into a rectangular lattice in the L–B film.

The AFM images in Fig. 2 (both *a* and *b* are 70 × 70 nm), obtained by scanning Chl *a* L–B films transferred under the same conditions with a homemade AFM, also show a well organized grain-structured L–B film. The AFM image in Fig. 2*c* (17.5 × 17.5 nm) also shows grains packed into a rectangular lattice in the L–B film. The force between the probing tip and the sample was held constant at 1 to 5 nN during the scanning. However, when this force is increased above 10 nN, we notice that the AFM tip causes the Chl *a* to form large aggregates with an average length of 1.50 μm (Fig. 2*d*). The shape of the aggregates is similar to the chains formed in the colloids of microcrystalline Chl *a* (12). Also, the average width (140 nm) of the aggregates is approximately within the range of the chain's width (12).

The distances estimated from the profiles obtained along four different directions (Fig. 3) are in good agreement with the distances obtained from the STM images. In Fig. 3*a*, the plots B and D show the grains with an average width of 3.00 ± 0.15 nm. The average distance between the two nearest maxima along these directions is 3.20 ± 0.15 nm. This distance is within the range of the grain width. However, the average distances between two maxima along the directions A and C (Fig. 3*b*) are much larger: 4.00 ± 0.15 and 5.60 ± 0.15 nm for A and C, respectively. The width of the grains is also much larger: 4.00 ± 0.15 & 6.00 ± 0.15 nm for A and C, respectively. One has to consider the plots A and C as diagonal profiles.

The organization of Chl *a* molecules at the air/water interface is important for the determination of the grain structure. Chapados and Leblanc (13) have proposed a model describing the organization of Chl *a* macrocycles in a mono-

The publication costs of this article were defrayed in part by page charge payment. This article must therefore be hereby marked "*advertisement*" in accordance with 18 U.S.C. §1734 solely to indicate this fact.

0027-8424/97/943504-3$2.00/0
PNAS is available online at **http://www.pnas.org**.

Abbreviations: Chl *a*, chlorophyll *a*; PS I, photosystem I; L–B, Langmuir–Blodgett; STM, scanning tunneling microscopy; AFM, atomic force microscopy.

*To whom reprint requests should be addressed.

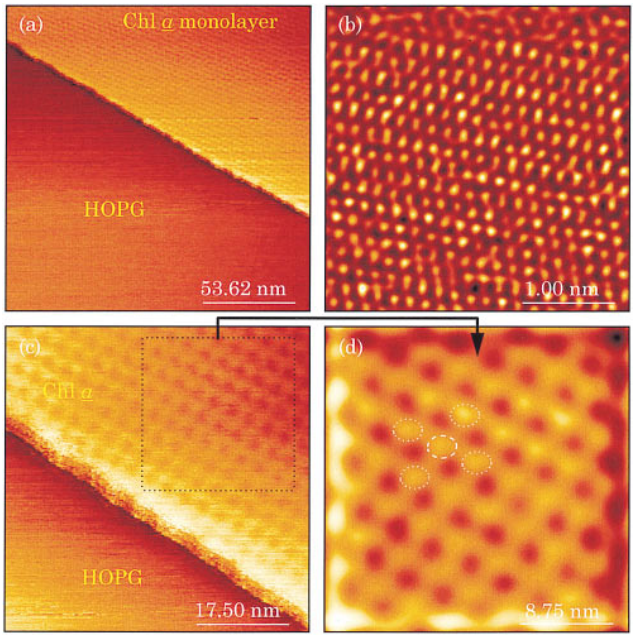

FIG. 1. STM images of one monolayer of Chl *a*. (*a*) 214.5 × 214.5 nm, (*c*) 70 × 70 nm, (*d*) 35 × 35 nm, and the graphite surface (*b*) 4 × 4 nm. The monolayer is transferred at a surface pressure of 20 mN/m onto graphite. The imaging was in air, and the tunneling current and the bias voltage were set to 0.1 nA and −300 mV, respectively.

layer compressed at 20 mN/m. They assume that Chl *a* macrocycles are tilted by 62.5° with respect to the water surface, and the distance between the Mg centers is about 0.70 nm (Fig. 4*a*). The value of this angle corresponds to the one estimated using polarized visible reflection of Chl *a* monolayers compressed to the same surface pressure (14). This orientation is supposedly maintained by H_2O molecules that form bridges between the Mg centers and the water surface (13). Considering the area of the porphyrin plane (1.987 nm^2), one can easily see the correlation between the molecular area

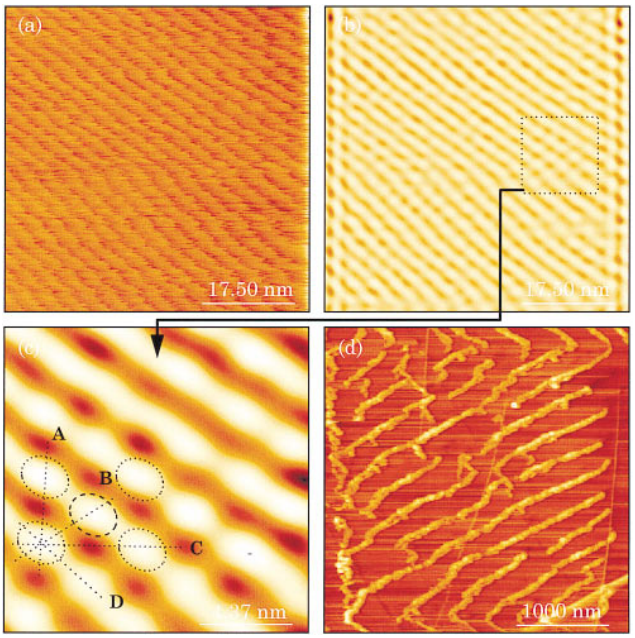

FIG. 2. AFM images of one monolayer of Chl *a* imaged with a probing force smaller than 5 nN (*a*) 70 × 70 nm, (*b*) 70 × 70 nm, (*c*) 17.5 × 17.5 nm and greater than 10 nN, and (*d*) 4 × 4 μm. The monolayer is transferred at a surface pressure of 20 mN/m onto graphite. The imaging was in air and in contact mode.

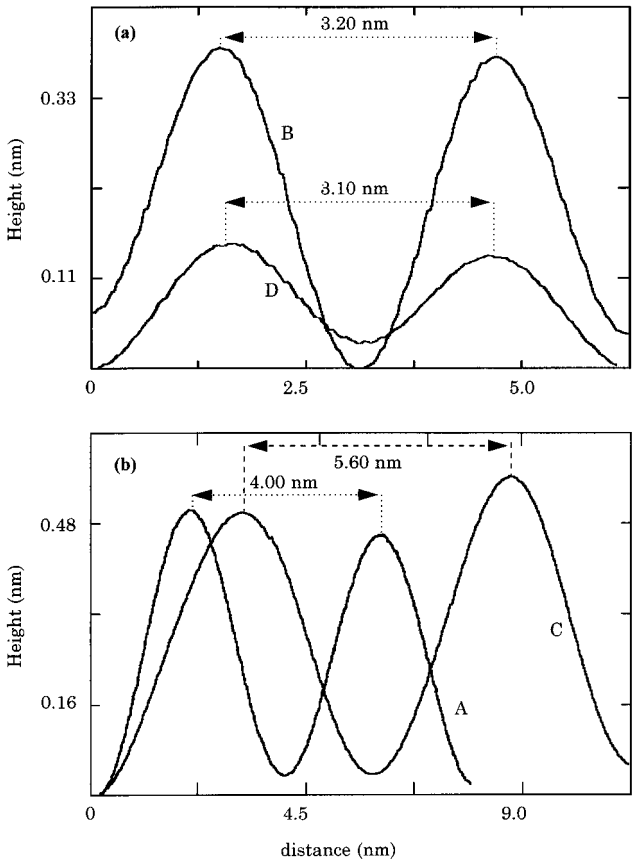

FIG. 3. Profiles of the Chl *a* grains along four different directions. The plots *a* and *b* correspond to the profiles of the grains along the directions B and D and A and C, respectively.

(0.980 nm^2 at 20 mN/m) and this orientation of the Chl *a* macrocycle. However, the STM and AFM images show a structure different than in the above model (13). The differences are related to the grain formation and the absence of the 0.70 nm gap between the Mg centers. Considering the rectangular shape and size of the grains, we consider the grains as dimers with (anti) parallel transition moments of the constituent monomers. In this dimer, the macrocycles are tilted toward each other by 30° with respect to the graphite surface (Fig. 4*b*). This angle of orientation corresponds to the angle calculated using the orientational properties of the reaction center triplet of PS II (15). However, this angle is much smaller than the one proposed by Chapados and Leblanc (13) and Okamura *et al.* (14). The change in the orientation angle (from 62.5 to 30°) probably has occurred during the transfer of the monolayer. This new arrangement of Chl *a* macrocycles corresponds with the width (3.00 ± 0.15 nm) and the heights (0.55 ± 0.05 nm) of the grains. It also explains the presence of the grooves observed between the grain rows in the AFM images. These features, missing in the STM images, probably are screened by the distribution of charge density (electronic component of the image).

The average distance estimated between two maxima (3.20 ± 0.15 nm) is in the range of the center-to-center distance (3.00 nm) calculated using transient absorption difference spectroscopy of the reaction center of PS II (16). It also should be noted that the 3.00 nm distance corresponds to the proposed distance between the Chl *a* accessory and P680. On the other hand, the distance between the Mg centers (1.20 ± 0.15 nm) within the dimer agrees with the calculated distance (≈1.00 nm) between centers of the Chl *a* identified as the special pair, P680 (17). It is possible that the distance between the Mg centers, in the compressed monolayer at the air/water

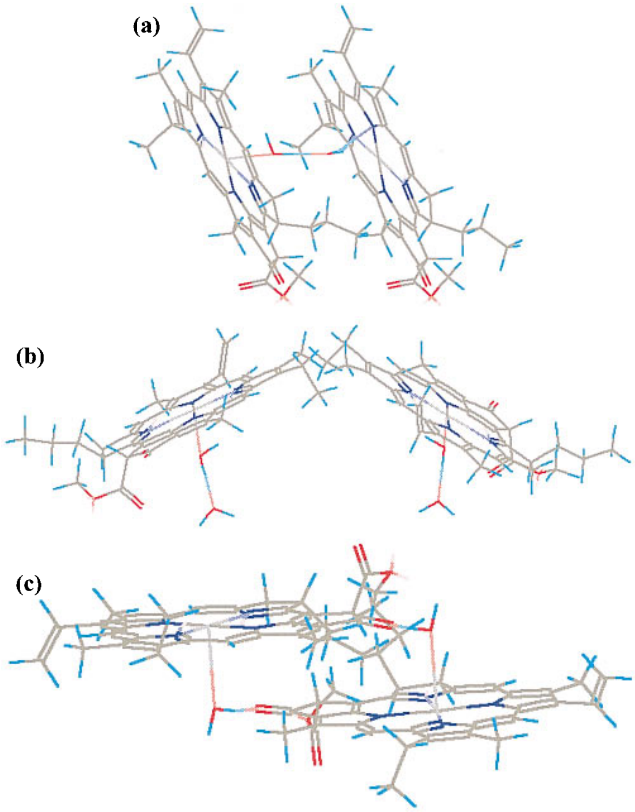

FIG. 4. Schematic representation of the structure and orientation of the Chl *a* in a L–B film (*a*) (see ref. 13), within the dimer imaged by the scanning probe microscopes (*b*), and in the C_2 symmetrical dimer (*c*) (see ref. 7).

interface, is smaller than 1.20 ± 0.15 nm. Considering the orientation angle estimated at the air/water interface (62.5°), the distance calculated between the Mg centers (0.70 ± 0.05 nm) corresponds to the gap estimated between the macrocycles (13). Compared with the special pair of the purple bacteria, Chl *a* molecules in the reaction center of PS II are weakly coupled to each other (18, 19). Therefore, the presence of a distance (1.20 nm), between the Mg centers in the dimer, can be considered as a reasonable argument for the weak coupling. Using the exciton formula of McRae and Kasha (20), and assuming a distance of 1.20 nm between the Mg centers, the dimer would be expected to absorb at 684 nm (21).

We consider that only a few H_2O molecules are holding together the stretched dimer, and their departure could easily alter the monolayer structure. This may result in a complete reorganization of the macrocycles. The proposed orientation resembles the proposed arrangement for the Chl *a* accessory molecules, which are most likely bound to histidines 118 of the D_1 and D_2 proteins (22). This similarity in organization is probably one of the reasons for the resemblance of the optical properties between the monolayer and PS II. In the light of these considerations, P680 is a dimer with a geometry different than the C_2-symmetrical (7) one shown in Fig. 4*c*.

The Chl *a* dimer formed in the monolayer, compressed at a surface pressure of 20 mN/m, may be a suitable model for the organization of P680, although *in vivo* Chl *a* interacts with the protein surrounding it. The packing of the Chl *a* dimers may be appropriate for producing systems with uniform charge density distribution. However, the distance between the dimers may slow charge transfer within the monolayer. Finally, H_2O is a key element in the formation of such dimers, and the aggregation of Chl *a* most likely begins with the dimer association.

This paper is dedicated to Dr. Pill Soon-Song for his 60th birthday. We would like to acknowledge Dr. J. J. Katz and R. A. Sachleben for useful discussions.

1. Rögner, M., Boekema, E. J. & Barber, J. (1995) *Trends Biochem. Sci.* **21,** 44–49.
2. Parson, W. (1991) in *Reaction Centers in Chlorophylls*, ed. Scheer, H. (CRC, Boca Raton, FL), pp. 1154–1172.
3. Katz, J. J. (1994) *Spectrum* **7,** 1–9.
4. Frackowiak, D., Zelent, B., Malak, H., Planner, A., Cegielski, R., Munger, G. & Leblanc, R. M. (1994) *J. Photochem. Photobiol. A* **78,** 49–55.
5. Katz, J. J., Bowman, M. K., Michalski, T. J. & Worcester, D. L. (1991) in *Chlorophyll Aggregation: Chlorophyll/Water Micelles as Models for in Vivo Long-Wavelength Chlorophyll in Chlorophylls*, ed. Scheer, H. (CRC, Boca Raton, FL), pp. 212–232.
6. Hann, R. A. (1990) in *Molecular Structure and Monolayer Properties in Langmuir–Blodgett Films*, ed. Roberts, G. (Plenum, New York), pp. 17–83.
7. Shipman, L. L., Cotton, T. M., Norris, J. R. & Katz, J. J. (1976) *Proc. Natl. Acad. Sci. USA* **73,** 1791–1794.
8. Zasadzinski, J. A. N. (1989) *BioTechniques* **7,** 174–187.
9. Ogletree, F. & Salmeron, M. (1990) *Prog. Solid State Chem.* **20,** 235–303.
10. Bustamante, C., Dorothy, A. E. & Keller, D. (1994) *Curr. Opin. Struct. Biol.* **4,** 750–760.
11. Hansma, H. G. & Hoh, J. H. (1994) *Annu. Rev. Biophys. Biomol. Struct.* **23,** 115–139.
12. Boussaad, S., De Rose, J. D. & Leblanc, R. M. (1995) *Chem. Phys. Lett.* **246,** 107–113.
13. Chapados, C. & Leblanc, R. M. (1983) *Biophys. Chem.* **17,** 211–244.
14. Okamura, E., Hasegawa, T. & Umemura, J. (1995) *Biophys. J.* **69,** 1142–1147.
15. Van Micghem, F. J. E., Satoh, K. & Rutherford, A. W. (1991) *Biochim. Biophys. Acta* **1058,** 379–385.
16. Schelvis, J. P. M., Van Noort, P. I., Aartsma, T. J. & Van Gorkom, H. J., (1994) *Biochim. Biophys. Acta* **1184,** 242–250.
17. Braun, P., Greenberg, B. M. & Scherz, A. (1990) *Biochemistry* **29,** 10376–10387.
18. Kwa, S. L. S., Eijckelhoff, C., van Grondelle, R. & Dekker, J. P. (1994) *J. Phys. Chem.* **98,** 7702–7711.
19. Michel, H. & Deisenhofer, J. (1988) *Biochemistry* **27,** 1–7.
20. McRae, E. G. & Kasha, M. (1964) *Fundamental Processes in Radiation Biology* (Academic, New York), pp. 23–42.
21. Kreutz, W. (1968) *Z. Naturforsch.* **23,** 520–527.
22. Kobayashi, M., Maeda, H., Watanabe, T., Nakane, H. & Satoh, K. (1990) *FEBS Lett.* **260,** 138–140.